*Bulletin de la Société Royale des Sciences de Liège, Vol. 80, 2011, p. 104 - 108*

# Pulsations in Wolf-Rayet Stars: Observations with *MOST**

André-Nicolas Chené[1,2,3] and Anthony F. J. Moffat[4]

[1] Departamento de Física, Universidad de Concepción, Chile
[2] Departamento de Física y Astronomía, Universidad de Valparaiso, Chile
[3] National Research Council of Canada, Herzberg Institute of Astrophysics, Canada
[4] Département de Physique, Université de Montréal, Canada

**Abstract:** Photometry of Wolf-Rayet (WR) stars obtained with the first Canadian space telescope *MOST* (Microvariability and Oscillations of STars) has revealed multimode oscillations mainly in continuum light. The latter suggest stellar pulsations could be a significant contributing factor to the mass-loss rates. Since the first clear detection of a pulsation period of P = 9.8h in WR123, two other stars have also shown periods of a few days, which must be related to stellar pulsations.

## 1 Introduction

The wind momentum ($\dot{M}\,v$) of the Wolf-Rayet (WR) stars is a factor $\sim$10 times higher than the radiative momentum outflow rate ($L/c$); radiation pressure doesn't seem to be sufficient to initiate the strong winds. Hence, another driving mechanism should be present near, or at the surface of the star. Theoretical work suggest that strange-mode pulsations (SMPs) are present in the envelope of hot and luminous stars with a large luminosity-to-mass ratio, where the thermal timescale is short compared to the dynamical timescale, and where radiation pressure dominates (Glatzel, Kiriadikis & Fricke 1993). Hence, the most violent SMPs are expected in classical WR stars, where SMPs manifest themselves in cyclic photometric variability with periods ranging from minutes to hours (Glatzel et al. 1999). However, this variability is expected to be epoch-dependent, with small amplitude, therefore, very difficult to detect from the ground. That is why the study of WR stars became one of the primary science drivers of the space telescope *MOST* (Microvariability and Oscillations of STars, Matthews et al. 1999, Walker et al. 2003). The *MOST* photometry is non-differential, but given the orbit, its thermal and design characteristics, experience has shown that it is a very photometrically stable platform even over long timescales (with repeatability of the mean instrumental flux from a non-variable target with V$\sim$11-12 to within about 1 mmag over a month).

*Based on data from the *MOST* satellite, a Canadian Space Agency mission, jointly operated by Dynacon Inc., the University of Toronto Institute for Aerospace Studies and the University of British Columbia, with the assistance of the University of Vienna.

## 2 Three First Stars Observed With *MOST*

Since its launch, *MOST* has observed one WR star per year. The first one is the famous WN8 type WR 123 (Lefèvre et al. 2005). Its light curve has a total amplitude of 10 mmag and the periodogram shows a significant peak at $\sim$ 2.45 c d$^{-1}$ (i.e. P$\sim$9.8 hours). Two quite different scenarios have been proposed to explain these observations. Townsend & MacDonald (2006) find that a deep, hot Fe opacity bump can lead to $g$-mode pulsations, but assumed a traditionally small stellar radius ($R_* \sim 2R_\odot$) compared to $R_* \sim 15R_\odot$, according to Crowther et al. (1995). As for, Dorfi, Gautschy & Saio (2006), they find that a cooler Fe opacity bump can produce SMPs, but had to assume significant hydrogen ($X_H$=0.35), compared to the observed value of 0.00. Both of these assumptions on the radius and on $X_H$ contradict what we know about this star, thus casting some doubt on their applicability.
On the second year was observed WR 103, a dust-making WR star of the Carbon sequence. No clear period could be found although the light curve shows clear variations with an amplitude of $\sim$5 mmag (Marchenko et al. 2006). Simultaneous spectroscopy has shown that the changes are coming from the continuum light and not at all from the emission lines, formed further away in the expanding wind.
Finally, WR 111 (WC5) was observed in 2006. Moffat et al. (2008) have found no coherent Fourier components above the 50 part per million level over the whole interval for frequencies f$<$10 c d$^{-1}$. Simultaneous spectroscopic observations reveal a normal level of stochastic clumps propagating in the wind, which has no effect on period detection.

## 3 WR 124

WR 124 is a runaway star (e.g. Moffat et al. 1998) in the cool-nitrogen sequence with type WN8h (Smith, Shara & Moffat 1996). Fig. 1 shows the entire *MOST* light curve of WR 124 (*upper*) and a control star (*lower*), binned for each *MOST* orbit. Although significant variations are seen on timescales longer than $\sim$a day, no such variations are seen on shorter timescales and binning allows one to increase the photometric point-to-point *rms* precision from $\sim$3 mmag before binning to $\sim$0.5 mmag after. Using Period04 (Lenz & Breger 2005), we found three main frequencies present in the light-curve; $\nu_1$=0.714$\pm$0.001 c d$^{-1}$, $\nu_2$=0.375$\pm$0.001 c d$^{-1}$ and $\nu_3$=0.200$\pm$0.004 c d$^{-1}$. Fig. 1 shows a time-frequency plot with straddled 10-day sampling. In this figure, we see that the maximum power shifts from one of the main frequency to the other. However, the only frequency present for most of the observations if $\nu_1$ (P$\sim$5.0 d). Simultaneous spectral monitoring gives a period of P$\sim$4.45 d. The spectral line-profile variability of WR 124 is very similar to the one observed for WR 123, although with a smaller amplitude. Since both these stars are of similar spectral types, the same type of pulsation may be present in each. Also, from previous ground-based observations, all the $\sim$10 relatively well-observed WN8 stars (and some other WNL) show a similar high degree of intrinsic variability (Antokhin et al. 1995, Marchenko et al. 1998), implying that all cool nitrogen-sequence WR stars may show similar behavior.

## 4 WR 110

WR 110 is in the mid-nitrogen sequence with type WN5-6b (Smith et al. 1996). Although to date it lacks any obvious binary signature, a comprehensive radial velocity search has not yet been carried out. However, WR 110 does have relatively high X-ray flux, with a significant hard component above 3 keV, compared to its lower-energy 0.5 keV emission, as seen in most WN stars (Skinner et al. 2002). The lower-energy component likely arises due to small-scale turbulent shocks in the wind, with velocity dispersion $\sim$100 km s$^{-1}$, as seen in virtually all WR-star winds (Lépine & Moffat

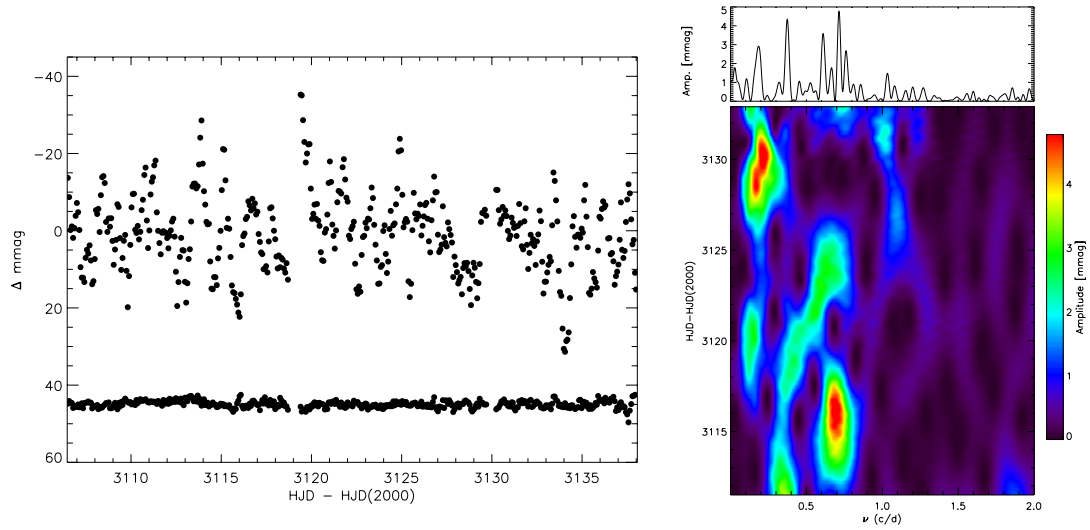


Figure 1: *Left*: *MOST* light curve of WR 124 in 101-minute MOST-orbit bins. *Right*: Fourier amplitude spectrum of the binned *MOST* light curve and Time-frequency Fourier plot with 10-day running windows in time.

1999) and other luminous hot stars (e.g. Eversberg, Lépine & Moffat 1998, Lépine & Moffat 2008). The former hard component implies velocities of at least $10^3$ km s$^{-1}$, which are more difficult to explain, without invoking an additional mechanism to provide such high speeds (e.g. accretion onto a low-mass companion or colliding winds with a massive companion). However, WR 110 emits normal thermal radio emission from its wind (Skinner et al. 2002), which lends little support for its binary nature. Recently St-Louis et al. (2009) have examined a northern sample of 25 WR stars for the presence of Corotating-Interaction Regions (CIRs) via large-scale variations exhibited on broad, strong emission lines. Some 20% of these stars show clear signatures of such effects, with WR 110 situated at the limit between those stars that show CIRs and those that do not. As we show in this investigation, it is possible and even likely, that WR 110's hard X-rays arise in the shocks produced by its CIRs rotating at velocities of $\sim 10^3$ km s$^{-1}$ relative to the ambient wind.

Fig. 2 shows the entire *MOST* light curve of WR 110 (*upper*) and a control star (*lower*), binned for each *MOST* orbit. Fig 2 also shows the Fourier spectrum for the *MOST* photometry (obtained using Period04; Lenz & Breger 2005). Here we see that the most significant peak occurs at a frequency of $\nu_1 = 0.245$ c d$^{-1}$ (P = 4.08 d), with harmonics of this frequency at, or close to, $n \times \nu_1$, with $n = 2$, 3, 4, 5 and 6. Examination of the light curve in Fig. 2 shows relatively sharp cusps occurring on this time scale (i.e. P = 4.08 d, starting at $t_0$ = HJD 2 454 270.27) in all seven cases but one (the third case), although even then there is a rise in brightness, though not cusp-like. The cusps have typical widths at the base of $\sim$ a day. Such cusps are clearly non sinusoidal, requiring a series of successive harmonics to reproduce them, as observed. Fig. 2 also shows a time-frequency plot with straddled 8-day (double the best period) sampling. This plot reveals that the 4.08-day period stands out at all times except just before the middle of the run and at the ends (where edge effects come into play). The former is compatible with the apparently suppressed third cusp, as noted above.

The most likely scenario to explain the low-amplitude ($\sim$1 %) 4.08 d periodicity and cusp-like behavior in the *MOST* light curve, along with mostly unrelated spectral variations, appears to be large-scale, emitting over-density structure rotating with the wind. An attractive scenario for this are the CIRs (or their source at the base of the wind) proposed for O star winds by Cranmer & Owocki (1996). Since there is no model of the changes of light caused by CIRs available in the literature, we

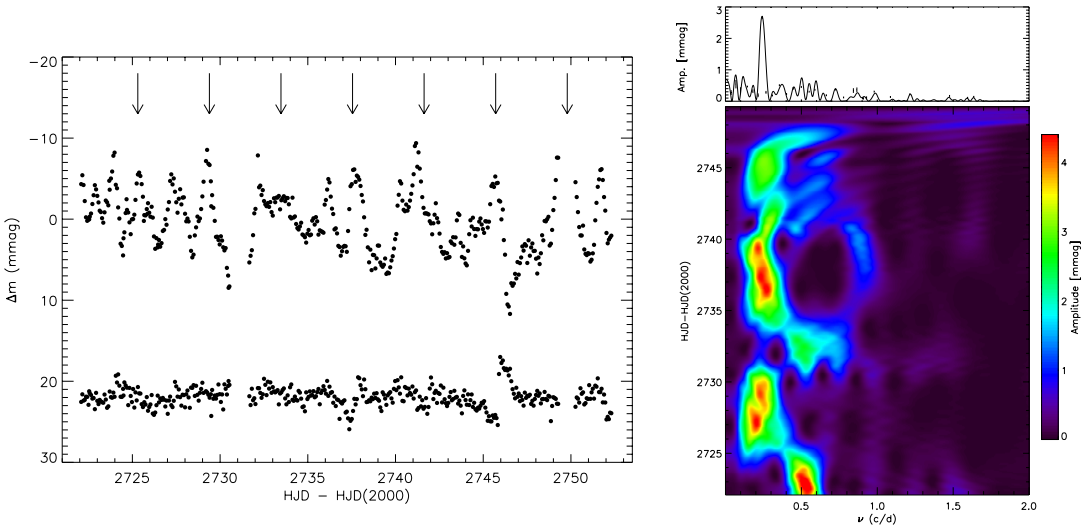


Figure 2: *Left*: *MOST* light curve of WR 110 in 101-minute MOST-orbit bins. The vertical lines indicate intervals of period 4.08 d starting at $t_0$ = HJD 2454270.31. *Right-Top*: Fourier amplitude spectrum of the binned *MOST* light curve. The highest peak refers to the adopted fundamental frequency corresponding to a period of P = 4.08 d. Harmonics are indicated at frequencies at multiples of 2 through 6 times fundamental. *Right-Bottom* : Time-frequency Fourier plot with 8-day running windows in time.

start with a very simplistic atmosphere model. First, we assume that the CIRs are continuum-emitting thermal sources, heated by the associated shock action created by a hot spot on the underlying rotating star with the ambient wind. Most of their emission must arise close to the star, where the ambient wind density is highest, as inspired by the simulations of Cranmer & Owocki (1996). Alternatively, the emission could arise in a hot spot at or close to the stellar surface, that produces the CIR. To simplify our calculations, we assume a point source located at some radius $R_s = \gamma R_*$ from the center of the star, with $\gamma > 1$ and $R_*$ being the stellar core radius. For simplicity (and following Cranmer & Owocki 1996) we assume the CIR to initiate at the stellar rotation equator.
In this scenario, the changes in the light-curve are caused by the assumed CIR-associated point source attenuated by the wind and seen at different angles with the line of sight as it rotates on the near side of the WR star. In this study, we use a simple WR wind model derived by Lamontagne et al. (1996) in the context of wind eclipses for WR + O systems. Hence, the change in magnitudes is defined as :

$$\Delta m \; = \; constant \; - \; 2.5 \log_{10} \left( I_{WR} + I_s \mathrm{e}^{-\tau} \right), \tag{1}$$

with arbitrary constant and where $I_{WR}$ is the intensity of the WR star and $I_s$, the intensity of the hot spot. Here the total opacity $\tau$ between the source and the observer, passing through the WR wind is :

$$\tau = k \int_{z_0}^{\infty} d\left(z/R_s\right) \left[ r^2 \left(1 - R_*/r\right)^{\beta} \right]^{-1} \tag{2}$$

where $z_0 = -(R_s \sin i) \cos 2\pi\phi$, with $R_s$, the radial position of the hot spot (or the region of light emission) and $i$, the inclination of the rotation axis relative to the observer. We allow for a WR wind with a $\beta$ velocity law, in which the actual $\beta$ value will be fitted. Taking the second cusp in the light curve in Fig. 2 as the cleanest, most representative form of the hotspot light curve, we fit the Equation 1 to match the data best, for i = 90° (to give the maximum effect). We consider two cases: (a) an optically thin point source, whose emission is isotropic in direction, and (b) an optically thick

source whose emission is maximum when seen perpendicularly to the stellar surface, dropping to zero when seen parallel to the surface (i.e. like pancakes on or near the stellar surface). In case (b), the values of $\gamma$ and $\beta$, which are always strongly coupled, tend to be slightly smaller than in case (a), since the projection factor in case (b) already provides a start (but only a start) to the correct form for the cuspy light curve, that requires less extended wind opacity to bring about the observed cuspy shape. All the best solutions for the thin and the thick cases are plotted in Fig. 3. Once again, this model is very simple, but its success is very encouraging. The next step would be to calculate the white-light emissivity of CIRs and to include their density distribution in the WR wind before calculating the light curve.

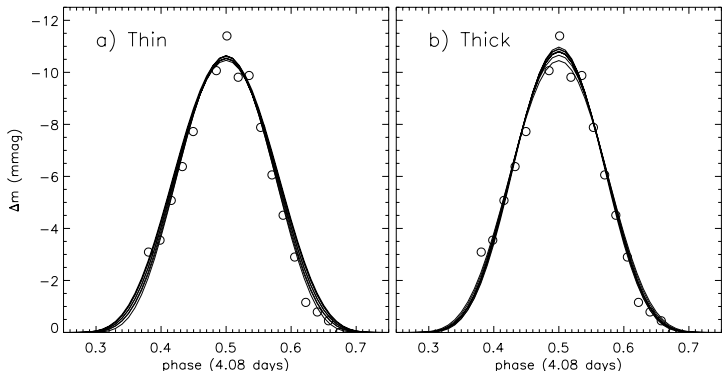


Figure 3: The data points refer to the second cusp indicated by a vertical line in Fig. 2. The curves indicate the best fits for (a) an optically thin point source and (b) an optically thick source (see text).

# References

Antokhin, I.I., Bertrand, J.-F., Lamontagne, R., Moffat, A.F.J., & Matthews, J. 1995, AJ 109, 817
Cranmer, S.R., & Owocki, S.P. 1996, ApJ 462, 469
Crowther, P.A.C., Smith, L.J., Hillier, D.J. & Schmutz, W. 1995, A&A 293, 403
Dorfi, E.A., Gautschy, A., & Saio, H. 2006, A&A 453, L35
Eversberg, T., Lépine, S., & Moffat, A.F.J. 1998, ApJ, 494 799
Glatzel, W., Kiriakidis, M., & Fricke, K. J. 1993, MNRAS 262, L7
Glatzel, W., Kiriakidis, M., Chernigovskij, S., & Fricke, K.J. 1999, MNRAS 303, 116
Lamontagne, R., Moffat, A.F.J., Drissen, L., Robert, C., & Matthews, J. M. 1996, AJ 112, 2227
Lefèvre, L., Marchenko, S.V., Moffat, A.F.J., et al. 2005, ApJ 634, L109
Lépine, S., & Moffat, A.F.J. 1999, ApJ 514, 909
Lépine, S., & Moffat, A.F.J. 2008, AJ 136, 548
Lenz, P., & Breger, M. 2005, CoAst 146, 53
Matthews, J.M., Kuschnig, R., Walker, G.H.A., et al. 1999, JRASC 93, 183
Marchenko, S.V., Moffat, A.F.J., Eversberg, T., Morel, T., Hill, G.M., Tovmassian, G.H. & Seggewiss, W. 1998, MNRAS 294, 642
Marchenko, S., Lefèvre, L., Moffat, A.F.J., et al. 2006, AAS 208, 4601
Moffat, A.F.J., Marchenko, S.V., Bartzakos, P., et al. 1998, ApJ 497, 896
Moffat, A.F.J., Marchenko, S.V., Zhilyaev, B.E., et al. 2008, ApJ 679, L45
Skinner, S.L., Zhekov, S.A., Güdel, M., & Schmutz, W. 2002, ApJ 572, 477
Smith, L.F., Shara, M.M., & Moffat, A.F.J. 1996, MNRAS 281, 163
St-Louis, N., Chené, A.-N., Schnurr, O., & Nicol, M.-H. 2009, ApJ 698, 1951
Townsend, R.H.D., & MacDonald, J. 2006, MNRAS 368, L57
Walker, G.H.A., Matthews, J., Kuschnig, R., et al. 2003, PASP 115, 1023